

Openspritzer: an open hardware pressure ejection system for reliably delivering picolitre volumes

Article (Published Version)

Forman, C J, Tomes, H, Mbobo, B, Burman, R J, Jacobs, M, Baden, T and Raimondo, J V (2017) Openspritzer: an open hardware pressure ejection system for reliably delivering picolitre volumes. Scientific Reports, 7 (1). ISSN 2045-2322

This version is available from Sussex Research Online: <http://sro.sussex.ac.uk/id/eprint/68763/>

This document is made available in accordance with publisher policies and may differ from the published version or from the version of record. If you wish to cite this item you are advised to consult the publisher's version. Please see the URL above for details on accessing the published version.

Copyright and reuse:

Sussex Research Online is a digital repository of the research output of the University.

Copyright and all moral rights to the version of the paper presented here belong to the individual author(s) and/or other copyright owners. To the extent reasonable and practicable, the material made available in SRO has been checked for eligibility before being made available.

Copies of full text items generally can be reproduced, displayed or performed and given to third parties in any format or medium for personal research or study, educational, or not-for-profit purposes without prior permission or charge, provided that the authors, title and full bibliographic details are credited, a hyperlink and/or URL is given for the original metadata page and the content is not changed in any way.

SCIENTIFIC REPORTS

OPEN

Openspritzer: an open hardware pressure ejection system for reliably delivering picolitre volumes

C. J. Forman¹, H. Tomes², B. Mbobo^{2,3}, R. J. Burman², M. Jacobs^{3,4,5}, T. Baden^{1,6} & J. V. Raimondo²

The ability to reliably and precisely deliver picolitre volumes is an important component of biological research. Here we describe a high-performance, low-cost, open hardware pressure ejection system (Openspritzer), which can be constructed from off the shelf components. The device is capable of delivering minute doses of reagents to a wide range of biological and chemical systems. In this work, we characterise the performance of the device and compare it to a popular commercial system using two-photon fluorescence microscopy. We found that Openspritzer provides the same level of control over delivered reagent dose as the commercial system. Next, we demonstrate the utility of Openspritzer in a series of standard neurobiological applications. First, we used Openspritzer to deliver precise amounts of reagents to hippocampal neurons to elicit time- and dose-precise responses on neuronal voltage. Second, we used Openspritzer to deliver infectious viral and bacterial agents to living tissue. This included viral transfection of hippocampal interneurons with channelrhodopsin for the optogenetic manipulation of hippocampal circuitry with light. We anticipate that due to its high performance and low cost Openspritzer will be of interest to a broad range of researchers working in the life and physical sciences.

The controlled delivery of picolitre to microliter volumes is of experimental utility across multiple research disciplines. Such scenarios include the targeted delivery of a wide range of pharmacologically active, genetic or infectious agents to biological preparations^{1–5}. Precise spatio-temporal control of drug delivery is often important. For example, pressurised ejection systems have been used to deliver neurotransmitters to individual dendritic spines that measure only 1–2 μm across and respond with millisecond-precision⁶. However, commercial pressure-ejection systems that provide the required accuracy are expensive, typically in the range of several thousands of pounds (See Supplementary Table 1). Here, we present “Openspritzer”, an Open Labware^{7,8} alternative, which can be built for ~£360 from off the shelf components and 3D printed parts.

Openspritzer (Fig. 1A,B) is designed around a fast switching solenoid under the control of an Arduino Nano microcontroller (Fig. 1C) or an externally generated 5 V Transistor-Transistor-Logic (TTL) pulse. Openspritzer controls the duration of a pulse of compressed air (hereafter referred to as a “puff”) delivered to a standard micro-injection pipette. Puff pressure is adjusted using a pressure regulator with a monitoring gauge (Fig. 1A₃) and puff duration is controlled either through an externally generated TTL command pulse (Fig. 1B₈) or through an internal control system set by a rotary encoder (Fig. 1A₂, cf. Fig. 1D). All instructions for assembly and operation of Openspritzer, the bill of materials (BOM) including possible suppliers, the 3-D model files for the external chassis and the heavily annotated microcontroller control code are provided (Supplementary Information).

In this study, we benchmarked Openspritzer against a commercial alternative and found that it has the same level of performance in terms of consistency and control of dose. We show this control by measuring the duration

¹School of Life Sciences, University of Sussex, Sussex, United Kingdom. ²Division of Physiology, Department of Human Biology, Neuroscience Institute and Institute of Infectious Disease and Molecular Medicine, Faculty of Health Sciences, University of Cape Town, Cape Town, South Africa. ³Division of Immunology, Department of Pathology, Institute of Infectious Disease and Molecular Medicine, Faculty of Health Sciences, University of Cape Town, Cape Town, South Africa. ⁴Immunology of Infectious Disease Research Unit, South African Medical Research Council, Cape Town, South Africa. ⁵National Health Laboratory Service, Sandringham, Johannesburg, South Africa. ⁶Institute for Ophthalmic Research, University of Tuebingen, Tuebingen, Germany. Correspondence and requests for materials should be addressed to C.J.F. (email: chrisforman@cantab.net) or T.B. (email: t.baden@sussex.ac.uk) or J.V.R. (email: joseph.raimondo@uct.ac.za)

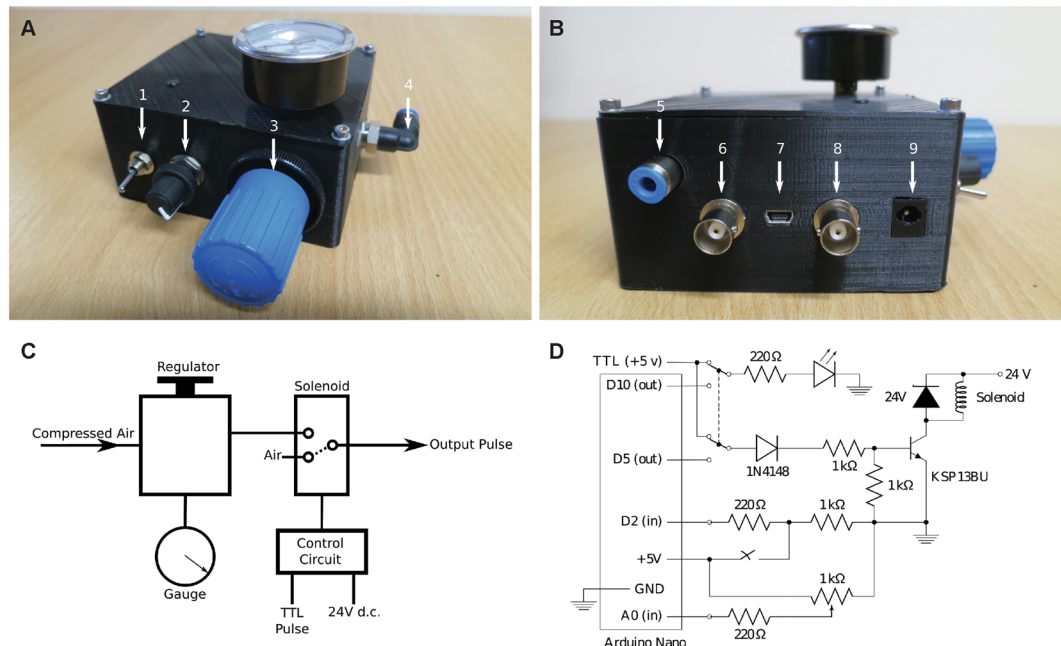


Figure 1. Openspritzer employs a fast switching solenoid to control the duration of a puff of compressed air. **(A)** Front panel view. Arrow 1: switch between external TTL pulse control or internal Arduino control. 2: potentiometer sets the internal pulse duration with feedback via light emitting diode (LED). 3: pressure regulator. 4: compressed air input port. **(B)** Back panel view. 5: compressed air output port. 6: Remote operation BNC connector (for a push-to-close SPST switch e.g. a footswitch). 7: USB port for +5 V Arduino power and software uplink. 8: TTL pulse input via BNC connector. 9: 24 V DC supply for the solenoid. **(C)** System schematic. The solenoid switches state when the +5 V TTL input is high, connecting the air input to the puffer output. When open the puffer output is connected to atmospheric pressure. The smallest achievable pulse time is less than 10 ms and limited by the solenoid switching speed. **(D)** Full circuit diagram. Internal or external control is selected via the Double Pole Double Throw (DPDT) switch. On internal control the pulse duration is selected by the potentiometer and flashes the LED to indicate the setting. The pulse is activated by a remote foot switch. The main solenoid circuit employs a darlington pair, represented as a single high gain transistor, to control the 114 mA solenoid via the low current Arduino pin 5 (40 mA max) and employs a number of protection diodes to prevent back emf from the solenoid from blowing the transistor or the Arduino.

and brightness of a puff of dye in water using a two-photon scanning fluorescence microscope. To demonstrate the utility of Openspritzer in a typical laboratory context we successfully performed a range of experiments in rodent and human brain slices involving the focal delivery of multiple different reagents including neurotransmitters, neurotransmitter analogues, bacterial extracts, viral vectors and whole live bacteria. This establishes Openspritzer as a reliable, precise and cost-effective means of delivering picolitre to microlitre volumes within the research environment.

Methods

Openspritzer construction. Openspritzer is built around a fast switching solenoid valve (Festo MHE2-MS1H-3/2G-M7) connected to a precision regulator (Festo LRP-1/4-4), which allows puff pressure control from 0 to 4 bar (Fig. 1). A typical line pressure of 1.4 bar gives rapid solenoid closure and a crisp cut off. A simple control circuit employs a low current (1 mA) 5 V signal to control a pair of transistors (Darlington pair) rated at 500 mA to open and close the high current solenoid (measured as 114 mA in a steady open state). Operation of the solenoid can be achieved *via* externally generated TTL pulses, (for example, PulseQ electrophysiology package (Funetics) running on Igor Pro (Wavemetrics) in conjunction with an ITC 1600) or *via* internally generated pulses controlled from an Arduino. The Arduino monitors a push-to-close Single Pole Single Throw (SPST) footswitch that can trigger either a single pulse whose duration is set *via* a potentiometer (single click), or a more sophisticated pre-programmed pulse train (double click). Full construction and operational details are included in the Supplementary Information.

Two-photon fluorescence microscopy. Puffer pipettes (3 to 5 Mohms tip resistance) were pulled from filamented borosilicate glass capillaries (1.2 mm outer diameter, 0.69 mm inner diameter; World Precision) and filled with 0.1% sulforhodamine 101 fluorescent dye from Sigma-Adrich. The Openspritzer or a World Precision Instruments Pneumatic Picopump PV 820 Picopump were connected to the pipette in turn, via a World Precision 1.2 mm microelectrode holder mounted on a micro-manipulator. Pulses were monitored under a two-photon scanning microscopy system (Movable Objective Microscope, Sutter⁹) equipped with galvanic scanners and a water immersion objective (W Plan Apochromat 20x/1,0 DIC M27, Zeiss), running off a Ti-Sapphire Laser

(Vision-S, Coherent) tuned to 927 nm. Fluorescence was detected through a Hamamatsu Photomultiplier filtered at HQ 630/60 (AHF). For image acquisition, we used custom-made software (ScanM, by M. Mueller, MPI, Martinsried and T. Euler, CIN, Tuebingen) running under Igor Pro (Wavemetrics). For time-precise measurement of dye ejection from the micropipette, scan amplitude of the laser was set to be near the point spread function of the optical system ($\sim 0.5 \mu\text{m}$ in the XY plane). This arrangement effectively allowed us to sample the same point at 42.7 kHz digitisation rate, which corresponds to 23.4 μs temporal resolution. Placing the sampling just beyond the tip of the electrode allowed precise measurement of the onset, duration and decay of the fluorescence pulses. Since dye is constantly injected into the scan region, photo bleaching during long pulses is not an issue. Notably, in the used configuration, the acquisition setup did collect data continuously but was switched off during the flyback fraction of the raster pattern at the end of each scan line (2 ms per line). Thus data was collected at 42.7 kHz in 1.6 ms bursts, with blind spots of approx 0.4 ms on each line. For simplicity, we therefore averaged the data over each scan line in the raster pattern effectively reducing temporal resolution to a single value per line, corresponding to 500 Hz. This arrangement was adequate to detect the onset and decay of a 10 ms puff of dye arising from opening the solenoid for 2 ms.

Brain slice preparation and electrophysiological recordings. Rat or mouse organotypic hippocampal slice cultures were prepared using a method similar to that described by Stoppini and colleagues¹⁰. Briefly, 7 day old male animals were sacrificed in accordance with South African national guidelines (South African National Standard: The care and use of animals for scientific purposes, 2008) with approval from the University of Cape Town Animal Ethics Committee. The brains were extracted and placed in 4°C Geys Balanced Salt Solution (GBSS), supplemented with 34.7 mM D-glucose. The hemispheres were separated and individual hippocampi were removed and immediately sectioned into 350 μm thick slices on a McIlwain tissue chopper. Slices were rinsed in cold dissection medium, placed onto Millicell-CM membranes and maintained in culture medium containing 25% Earle's Balanced Salt Solution, 50% Minimal Essential Medium, 25% heat-inactivated horse serum, glucose, and B27 (Invitrogen). Slices were incubated at 36°C in a 5% CO_2 humidified incubator. Slices were cultured for at least 7 days prior to performing electrophysiological recordings. For the optogenetic and BCG experiments, slices were inoculated using Openspritzer two days post culture, with a further week allowed for successful infection to occur.

For rat acute slices male animals between 14 to 21 days old were decapitated with institutional ethical approval (as above). The rat brain was extracted and quickly placed in a 50% sucrose cutting solution bubbled with carbogen gas (95% oxygen and 5% carbon dioxide). The cutting solution composed of (in mM): NaCl (60); KCl (3); NaH_2PO_4 (1.2); NaHCO_3 (23); D-glucose (11); MgCl_2 (3); CaCl_2 (1) and sucrose (120). 400 μm horizontal hippocampal slices were cut using a vibrating microtome. Slices were then transferred to a submerged chamber containing carbogen bubbled standard artificial cerebro-spinal fluid (aCSF). The composition of the aCSF was (in mM): 120 NaCl, 3 KCl, 2 MgCl_2 , 2 CaCl_2 , 1.2 NaH_2PO_4 , 23 NaHCO_3 , and 11 D-glucose. Slices were first kept at between 35–37°C for 20 minutes and then left to stand at room temperature (20–25°C) for a further 40 minutes. For human brain slices, brain tissue from temporal cortex was obtained from a 13 year old patient diagnosed with mesial temporal sclerosis and who was undergoing an elective left temporal lobectomy procedure at Red Cross Children's Hospital to treat refractory epilepsy. Ethical approval was granted by the University of Cape Town Human Research Ethics Committee (HREC 533/2013) according to institutional guidelines. Informed consent from both the patient and the patient's parents was obtained in written form in order to use the tissue for research purposes. The brain tissue was transported in cold 50% sucrose cutting solution equilibrated with carbogen gas. The pial covering was removed and the tissue cut into 400 μm using a similar method as described for the acute rat brain slice preparation.

For electrophysiological recordings, brain slices were transferred to a recording chamber and continuously superfused with 95% O_2 /5% CO_2 bubbled aCSF, heated to 32°C. The pH was adjusted to be between 7.35 and 7.40 using NaOH. For puffing either glutamate (100 μM), GABA (100 μM), muscimol (45 μM) acquired from Sigma and dissolved in standard aCSF or Tuberculin Purified Protein Derivative (PPD), Statens Serum Institute (Copenhagen, Denmark) 1 mg/ml in phosphate buffered saline (pH 7.38) were used. In a subset of the glutamate puffing experiments, as well as the PPD experiment, tetrodotoxin (1 μM), was added to the bath aCSF. Both patch and puffer pipettes (3 to 5 Mohms tip resistance) were pulled from filamental borosilicate glass capillaries (1.2 mm outer diameter, 0.69 mm inner diameter; Harvard Apparatus), using a horizontal puller (Sutter P-1000). For whole-cell recordings, pipettes were filled with an internal solution containing the following (in mM): 120 K-gluconate, 4 Na_2ATP , 0.3 NaGTP , 10 Na_2 -phosphocreatine, 10 KCl, and 10 4-(2-hydroxyethyl)-1-piperazineethanesulfonic acid. (HEPES). Osmolarity of internal solutions was adjusted to 290 mOsm and the pH was adjusted to 7.38 with KOH. Hippocampal neurons were visualised under a 40x water-immersion objective on a Zeiss Axioskop upright microscope and targeted for recording. Patch-clamp recordings were made using an Axopatch 200B amplifier (Molecular Devices) and digitised using an InstruTECH ITC 1600 controlled by the PulseQ electrophysiology package (Funetics) running on Igor Pro (Wavemetrics). Only recordings with an access resistance of <20 MOhms were included. Samples were acquired at 2 KHz and low-pass filtered at 2 KHz. PulseQ and the ITC 1600 were used to generate the 5 V TTL pulses for driving the Openspritzer. Micromanipulators, (Luigs Neumann, SM-1) were used to position both patch and puffer glass micropipettes. For optogenetics experiments, light was delivered using a 488 nm high powered LED (Thorlabs).

Immunohistochemistry and confocal microscopy. For immunohistochemistry, slices were rinsed with PBS (pH 7.4) at room temperature, followed by a 15 min wash in -20°C methanol. Following a 2nd rinse in PBS, slices were fixed in 4% paraformaldehyde in PBS for 1 hour at room temperature. After a further PBS wash, tissue was incubated at 4°C with blocking buffer (1% bovine serum albumin in PBS) for 1 hour. Slices were then incubated with rabbit β -tubulin III neuron specific antibody (dilution 1:1000) for 48 hours at 4°C. After 3 PBS washes,

slices were incubated overnight with goat anti-rabbit cy3 secondary antibody (dilution 1:1000). BCG-GFP and ChR2-YFP were imaged directly without an antibody raised against either fluorophore. The images of ChR2-YFP were made from a live organotypic brain slice whilst the BCG-GFP and neuronal staining were acquired from fixed tissue as described above. Confocal images were acquired using a Zeiss Axiovert 200 M LSM 510 Meta Confocal Microscope.

Results

Openspritzer control over dose delivery matches that of a leading commercial alternative. To directly assess the temporal precision and reliability of Openspritzer we visualised fluorescent dye puffs from a sharp microelectrode using a custom-built two-photon microscope. The images presented in Fig. 2A were taken from a puff that reached maximum intensity using a wide area scan. To achieve measurements of puffs with suitable time resolution we restricted the scan area to a region near the microscope's point spread function immediately adjacent to the pipette mouth (Fig. 2A, rectangles). This restriction in scan size yielded an effectively continuous reading of brightness at a single point and with a time resolution that is limited solely by the digitisation of the photomultiplier tube signal (42.7 kHz). However, for simplicity, we averaged the data over each 2 ms scan line to yield an effective sampling rate of 500 Hz. In this way we could reliably and precisely capture the on/off millisecond time scale of the wave front of the dye and meaningfully understand the true nature of the puff profiles of the commercial and bespoke hardware as a function of the duration of the command pulse.

A set of command pulses of 2–1000 ms duration were delivered to Openspritzer, and corresponding pulses were recreated using the built-in rotary encoder and footswitch activation of a Picopump, a widely used commercial device. The shortest command pulse which reliably generated a detectable puff for Openspritzer was 2 ms, compared to the lowest possible manual setting of 4 ms for Picopump. Fluorescence profiles of different command-duration puffs are shown in Fig. 2B₁,C₁ for Openspritzer and Picopump, respectively. The same data is shown again in log-log space to highlight details of shorter pulses (Fig. 2B₂,C₂). Overall, both devices behave in a very similar way in terms of providing effective and near linear control over the total dosage. For commands less than 15 ms the total puff duration is near constant (Fig. 2D), while peak fluorescence linearly follows the command duration (Fig. 2E). After this point, both puff duration and peak fluorescence grow in proportion to command duration until about 50–100 ms. For commands longer than 100 ms, the peak fluorescence remains constant while pulse duration continues to follow command duration (Fig. 2D). These relationships remain stable for quantification of area under the curve which combines both peak intensity and duration in a single metric (Suppl. Fig. S1). Finally, we compared the consistency of dose delivery by quantifying peak intensity reached during 30 consecutive pulses of 10 ms command duration (Fig. 2F). Here, both devices delivered very similar control (S.D.: 0.059 and 0.048 for Openspritzer and Picopump, respectively). Taken together, Openspritzer reliably delivered well defined doses of reagent to a level of control near indistinguishable to that of a leading commercial alternative. While each pulse train was taken with the same micropipette, input line pressure and connecting hoses, differences in absolute fluorescence arose. These were likely due to small variations in the positioning of the sample point on successive takes and possible differences in output pressures across the two devices.

Openspritzer controls neural activity by delivering neurotransmitters with millisecond precision. To determine the reliability and precision of Openspritzer for delivering controlled puff volumes in the context of a typical life-sciences experiment, we performed whole-cell patch clamp recordings on mouse hippocampal neurons *in-vitro* (Fig. 3). We then used Openspritzer to deliver precise volumes of neurotransmitter while monitoring the voltage response of the recorded neuron in current-clamp mode. Openspritzer was connected to a glass puffer pipette positioned within 30 μ m of the recorded cell's soma. Line pressure was adjusted to approximately 1.4 bar while puff duration was controlled *via* externally delivered TTL pulses. 20 ms doses of glutamate (100 μ M) reliably evoked excitatory postsynaptic potentials (EPSPs) and action potentials (Fig. 3A, top). Similarly, action potential activity elicited via somatic current injection could be suppressed by 20 ms puffs of γ -Aminobutyric acid (GABA, 100 μ M) a neurotransmitter that acts in an inhibitory fashion in these neurons (Fig. 3A, bottom). Openspritzer also reliably converted TTL trains of differing frequency into trains of glutamate puffs to elicit trains of EPSPs (Fig. 3B). Here we adjusted the line pressure so that a single puff of glutamate was insufficient to elicit an action potential. 2 Hz or 5 Hz trains of puffs did not evoke an action potential, however, a 10 Hz train resulted in sufficient summation and thus action potential generation. Next, we sought to quantify the reliability and precision of Openspritzer by performing multiple recording sweeps where the timing and duration of TTL driving pulses were kept constant. Here, ten consecutive puffs of 20 ms duration each resulted in ten near identical EPSP waveforms (Fig. 3C). Moreover all EPSPs occurred within 1 ms of each other relative to the command pulse (S.D. 0.4 ms), with a similar consistency in EPSP amplitudes (13.8 ± 0.4 mV). To test the effect of command duration on effective dose delivery, we next applied puffs of increasing duration from 10 to 100 ms in 10 ms steps (Fig. 3D). Here, each additional 10 ms increase in duration produced a clear increase in both EPSP duration and amplitude. These results confirm the reliability and precision of Openspritzer for delivering small doses of an agent to a widely used biological sample in a controlled manner.

Openspritzer demonstrates benzodiazepine enhancement of GABA_AR signalling in multiple systems including a human neuron. Having established Openspritzer as a reliable tool for high-fidelity delivery of reagents we next explored the efficacy of the benzodiazepine diazepam in positively modulating GABA_AR signalling in three different tissue preparations: rat organotypic, rat acute and human brain slices. Using Openspritzer to deliver 20 ms puffs of the selective GABA_A receptor agonist muscimol (45 μ M) resulted in seconds-long inhibitory postsynaptic potentials (IPSPs) in recorded neurons from all three preparations. The addition of 35 μ M diazepam to the bath media resulted in a consistent increase in the size of muscimol-induced IPSPs. In CA3 pyramidal neurons from rat organotypic slices IPSPs significantly increased in amplitude from

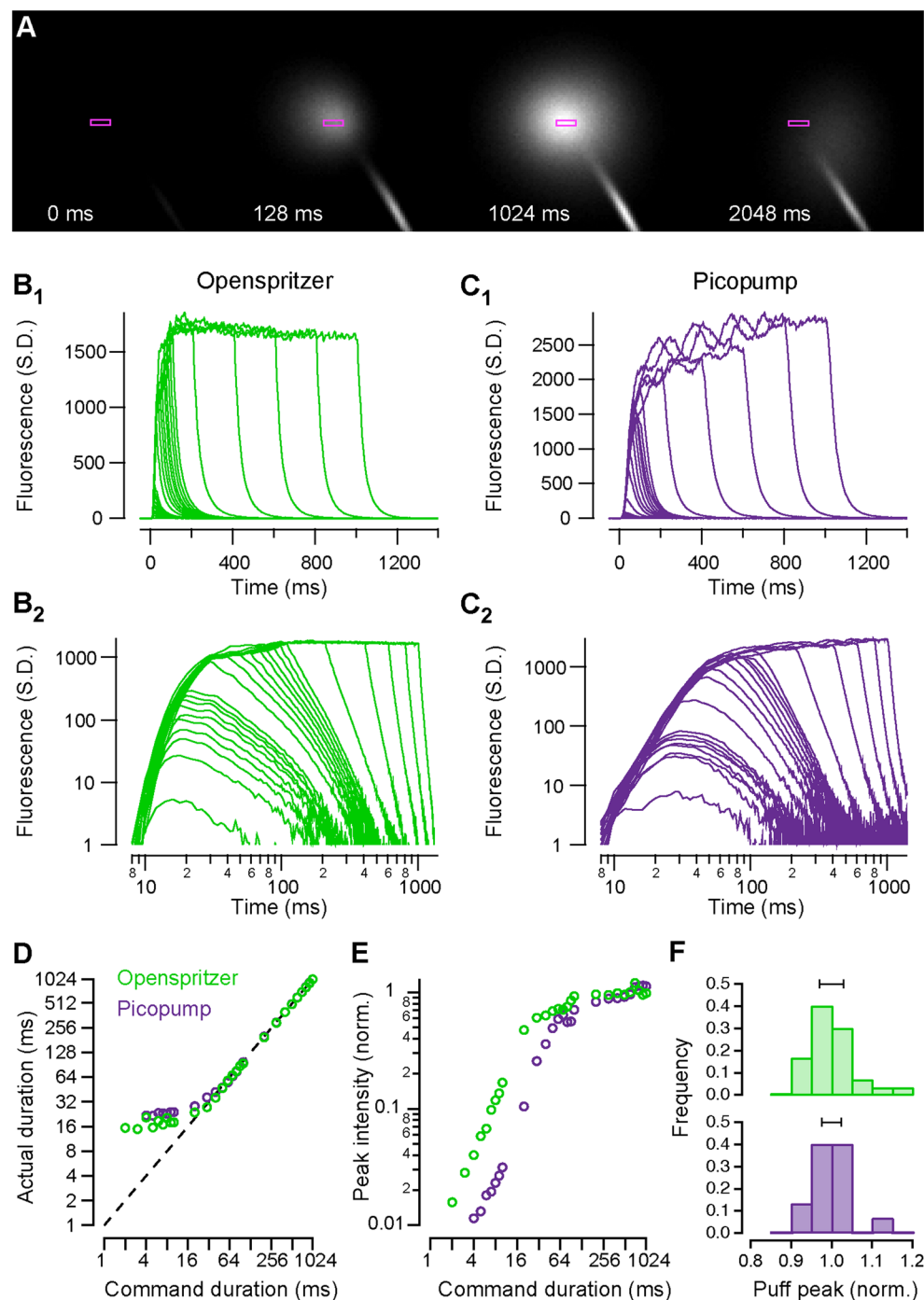


Figure 2. Two-photon imaging of fluorescent puff dynamics demonstrates comparable performance between Openspritzer and Picopump, a commercial alternative. Reducing the scanning motion of a two-photon scanning microscope to movements within the point spread function enabled time-precise imaging of fluorescent pulses emitted by either the Openspritzer or the Picopump. **(A)** Scanning image of a 100 ms Openspritzer pulse. **(B₁ and B₂)** A train of 27 puffs generated by Openspritzer ranging from 2 ms to 1000 ms command duration. **(B₁)** is a linear plot and **(B₂)** is a log-log plot of the same data. **(C₁ and C₂)** A train of 25 puffs generated by Picopump ranging from 4 ms to 1000 ms command duration. **(C₁ and C₂)** are linear and log-log plots, respectively. The original command durations were in 3 groups of 1 to 9 ms in 1 ms intervals, 10 to 90 ms in 10 ms intervals and 100 to 1000 ms in 200 ms intervals. **(D)** Puff duration, measured from the onset of the initial phase of the fluorescent pulse to decay onset plotted against command duration. **(E)** Normalised maximum peak intensity plotted against command duration, normalised to the average maximum value of the last nine puffs. **(F)** Histogram of the normalised maximum peak intensities of a train of thirty 10 ms puffs for Openspritzer and Picopump (black bars indicate SD). Openspritzer in green, Picopump in purple (**B–F**). All trials were taken with the same micropipette.

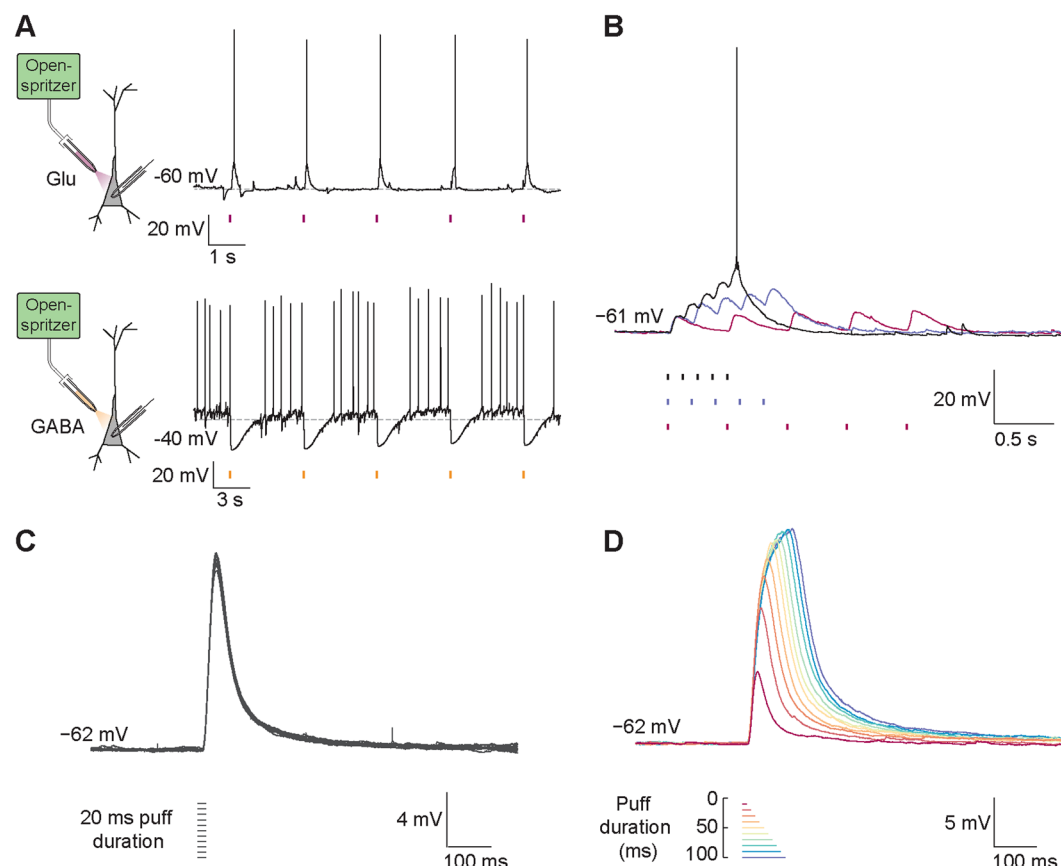


Figure 3. Openspritzer delivers neurotransmitters with millisecond precision to control neural activity. (A) Whole-cell patch clamp recordings in current clamp mode were performed on CA3 hippocampal pyramidal cells. Openspritzer was used to deliver 20 ms puffs of either glutamate (100 μ M), top, magenta, or GABA (100 μ M), bottom, orange, to the soma of recorded cells. A separate micropipette was used for each neurotransmitter. Membrane voltage recordings demonstrate that Openspritzer-applied glutamate reliably evoked EPSPs and action potentials (top). Similarly, GABA application reliably suppressed action potential activity elicited by somatic current injection (bottom). (B) In the same cell as in the top panel of 'A', driving pressure was adjusted so that a single 20 ms glutamate puff was insufficient to trigger an action potential. 2, 5 and 10 Hz application (magenta, blue and black) of 20 ms glutamate puffs resulted in distinguishable trains of EPSPs. The EPSPs in response to the 10 Hz train summated sufficiently to generate an action potential. (C) In separate recordings with a different micropipette and in the presence of 1 μ M tetrodotoxin to reduce synaptic noise, 10 sweeps including 20 ms glutamate puffs applied after 500 ms produced almost identical EPSPs demonstrating the precise timing of Openspritzer and highly conserved puff volumes. Traces were not rise-time or peak aligned. (D) Puffs of increasing duration from 10 to 100 ms in 10 ms steps resulted in EPSPs of increasing duration and amplitude.

5.9 ± 1.0 mV to 8.9 ± 0.9 mV (mean \pm SEM), $N = 6$ cells, $P = 0.03$, wilcoxon matched-pairs test (Fig. 4A). In layer V pyramidal cells from rat entorhinal cortex acute slices the addition of diazepam increased mean IPSP size from 9.8 ± 0.9 mV to 13.0 ± 1.3 mV, $N = 7$ cells, $P = 0.007$, paired t-test (Fig. 4B). In a novel demonstration of the action of diazepam in human GABAergic signalling, diazepam enhanced mean IPSP size in a recording from a layer V temporal cortex from 11.6 mV to 16.0 mV (Fig. 4C). This data is consistent with the known effects of diazepam and further demonstrates the utility of Openspritzer for gathering high-quality data.

Openspritzer reveals Tuberculin Purified Protein Derivative depolarization of hippocampal neurons.

To explore possible implications of *Mycobacterium tuberculosis* infection of the central nervous system we performed an additional experiment using Openspritzer. Specifically, we set out to determine whether Tuberculin Purified Protein Derivative (PPD), an extract from *Mycobacterium tuberculosis*, has any acute effects on the membrane potential of hippocampal neurons. Application of PPD using 20 ms puffs directed toward the somata of CA3 pyramidal neurons modestly but significantly depolarised hippocampal CA3 pyramidal neurons (Fig. 5A). The maximum PPD-induced depolarisation was 1.8 ± 0.5 mV (mean \pm SEM), $N = 5$, $P = 0.027$, t-test. To elicit this response the puffer pipette was typically placed close to the cell soma ($< 5 \mu$ m). Therefore, to exclude potential artefacts caused by physical perturbation of the neurons by the puff, aCSF was applied in a set of control cells. The application of aCSF in a similar manner to the PPD puffs did not result in any observable changes to the neuronal membrane potential

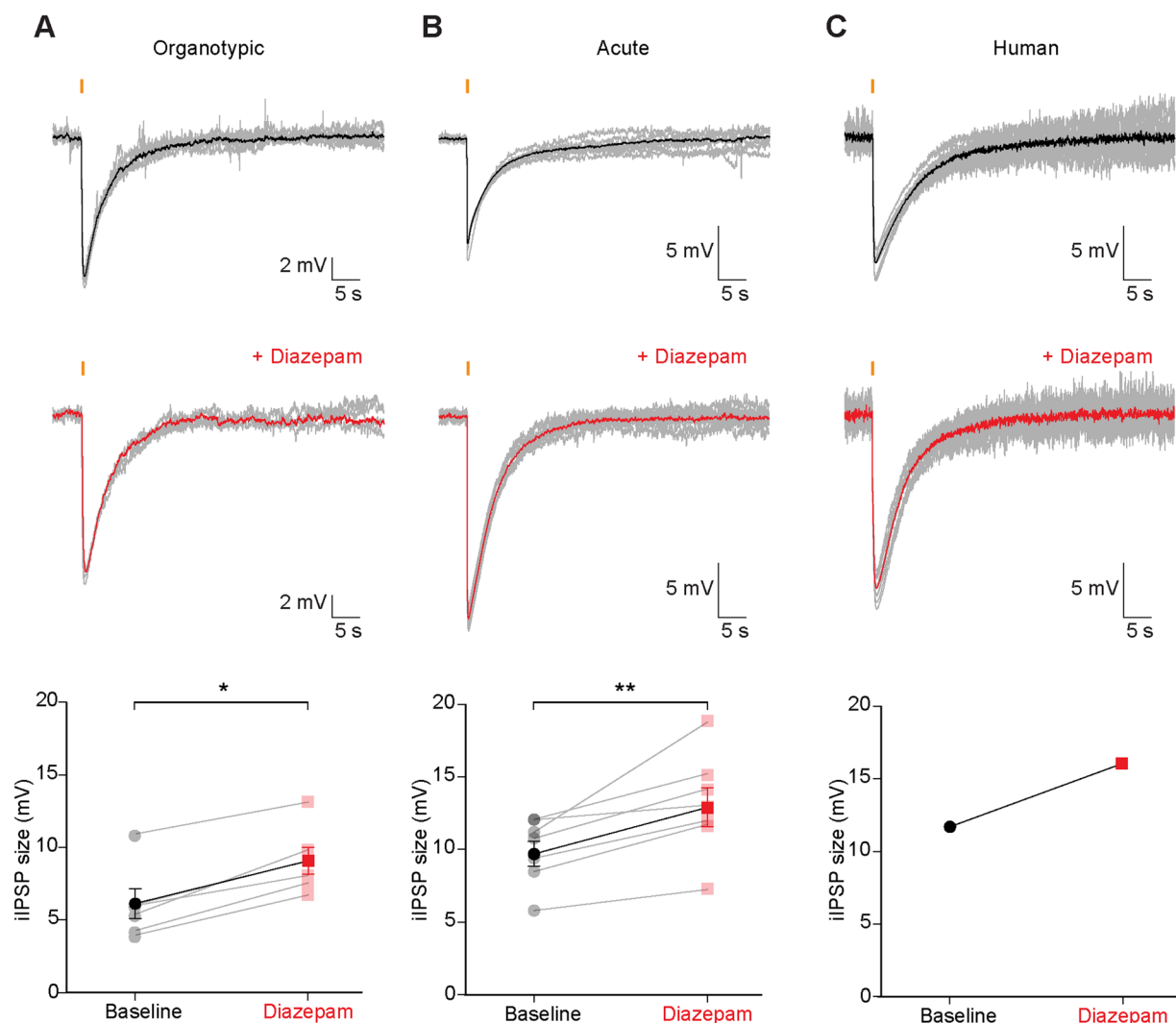


Figure 4. Openspritzer demonstrates benzodiazepine enhancement of GABA_AR signalling in multiple systems including a human neuron. **(A)** Diazepam increases the size of muscimol-induced inhibitory postsynaptic potentials in pyramidal cells from rat organotypic hippocampal brain slices. Whole-cell patch-clamp recordings were made from CA3 pyramidal cells. Current was injected to maintain a resting voltage of -60 mV. Top, 1 minute long recording sweeps (grey, mean response in black) where Openspritzer was used to deliver 20 ms pressurised puffs of muscimol ($45 \mu\text{M}$, orange bar) to selectively activate GABA_ARs. Traces are not rise-time aligned demonstrating the temporal fidelity of Openspritzer. Middle, addition of diazepam (DZP $35 \mu\text{M}$) to the aCSF resulted in a potentiation of the IPSP. Bottom, population data demonstrates that the size of muscimol-induced IPSPs increased after application of diazepam. **(B)** As in 'A', diazepam had a similar effect on muscimol-induced IPSPs in recordings made from entorhinal cortex layer 5 pyramidal cells in acute brain slices prepared from juvenile rats (P14–P21). **(C)** Muscimol-induced IPSPs are also enhanced by diazepam in a layer 5 pyramidal cell from resected human temporal cortex. * $p < 0.05$, ** $p < 0.01$, t-test.

(max. change in potential 0.11 ± 0.01 mV, $N = 5$, $P = 0.56$, t-test, Fig. 5B). This data demonstrates the usefulness of Openspritzer by revealing a previously undescribed effect of Tuberculin PPD on neurons.

Openspritzer is suitable for delivering infectious agents including viral delivery of opsins for optogenetics.

Finally we sought to verify the utility of Openspritzer for spatially localised microinjection of infectious agents into organotypic mouse brain slices. Innoculated agents included either adeno-associated virus serotype 1 (AAV1) carrying genes for channelrhodopsin-2 (ChR2) fused to yellow fluorescent protein (YFP) or *Mycobacterium bovis* (BCG) expressing green fluorescent protein (GFP). As before, a glass micropipette was partially filled with either infectious agent as well as a dye (fast green 0.1%) to aid visualisation. The puffer pipette was carefully lowered into the tissue using a Leitz micromanipulator. Under microscopic visualisation the infectious agents were microinjected into the brain slice parenchyma using 20 ms puffs commanded via a foot pedal (Fig. 6A). Spatial precision depended on the strength and duration of applied puffs. Viral DNA included the double-floxed sequence for ChR2-YFP driven by the elongation factor 1 promoter. Innoculation of

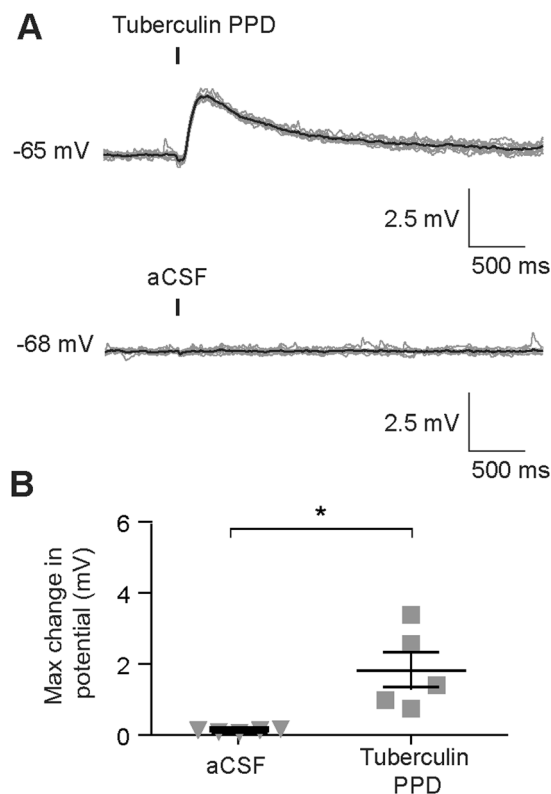


Figure 5. Application of Tuberculin Purified Protein Derivative (PPD) using Openspritzer causes neuronal depolarization of hippocampal neurons. Whole-cell current clamp recordings were performed from CA3 hippocampal pyramidal neurons to explore the effect of directly applied Tuberculin PPD. **(A)** 10 sweeps (grey) demonstrate a modest depolarization in response to 20 ms puffs of Tuberculin PPD directed at the cell soma. Mean response in black. **(B)** Application of aCSF as a control did not result in changes to membrane potential. **(C)** Population data depicts this statistically significant difference, $*p < 0.05$, t-test.

organotypic slices prepared from transgenic mice constitutively expressing cre recombinase under the Glutamic Acid Decarboxylase type 2 promoter (GAD2-cre) resulted in selective expression of ChR2-EYFP in GABAergic interneurons (Fig. 6B). Targeted whole-cell patch clamp recordings from ChR2-EYFP expressing cells revealed that delivery of 488 nm light reliably evoked action potentials, confirming successful expression of ChR2 (Fig. 6C, top). Inhibitory postsynaptic potentials could be recorded from neighboring pyramidal neurons during light activation demonstrating the selective activation of inhibitory circuitry. This shows the utility of Openspritzer for viral transfection in optogenetic experiments. Finally, we used Openspritzer to successfully inoculate brain slices with BCG-GFP (Fig. 6D) further demonstrating the utility of Openspritzer for enabling a wide array of potential biological experiments.

Discussion

Inspired by similar initiatives within the broader open hardware and open labware movement^{7,11}, we present Openspritzer, an open hardware pressure ejection system, which can be constructed from off the shelf components.

To assess the performance of Openspritzer we used data from two-photon imaging experiments to show that the dosage of reagents delivered in a puff can be effectively controlled by modifying the duration for which the solenoid valve is open. There are two ways in which dosage can be controlled by command duration, which is best understood by noting that for any given pressure and pneumatic set up, there is a maximum flow rate of reagent that can be attained. For short pulses, control consists of quenching the build up to the maximum flow rate before it can reach a peak. For longer pulses the dosage is simply controlled by how long the maximum flow rate is sustained. These two very different regimes give a different degree of sensitivity over the precise quantity of reagent that can be delivered by varying puff duration. At a pressure of 1.4 bar, the command duration at which the switch over between these two regimes occurs is 20 ms and 60 ms for the Openspritzer and Picopump, respectively. It is likely that the precise onset of the switch between the regimes is sensitive to the pressure within the system. We also observed oscillations in the steady state flow for both the Openspritzer and Picopump, however the oscillations were much larger for the commercial system in this case, which may be down to a variety of factors including the precise shape of the pipette, although this discrepancy will vanish at even longer timescales still, as any oscillations would tend to average out over time, regardless of their amplitude.

There are two key differences in behaviour between the Openspritzer and Picopump. The first is the lateral offset between the normalised peak intensities in Fig. 2E. This difference suggests that Picopump may be capable of

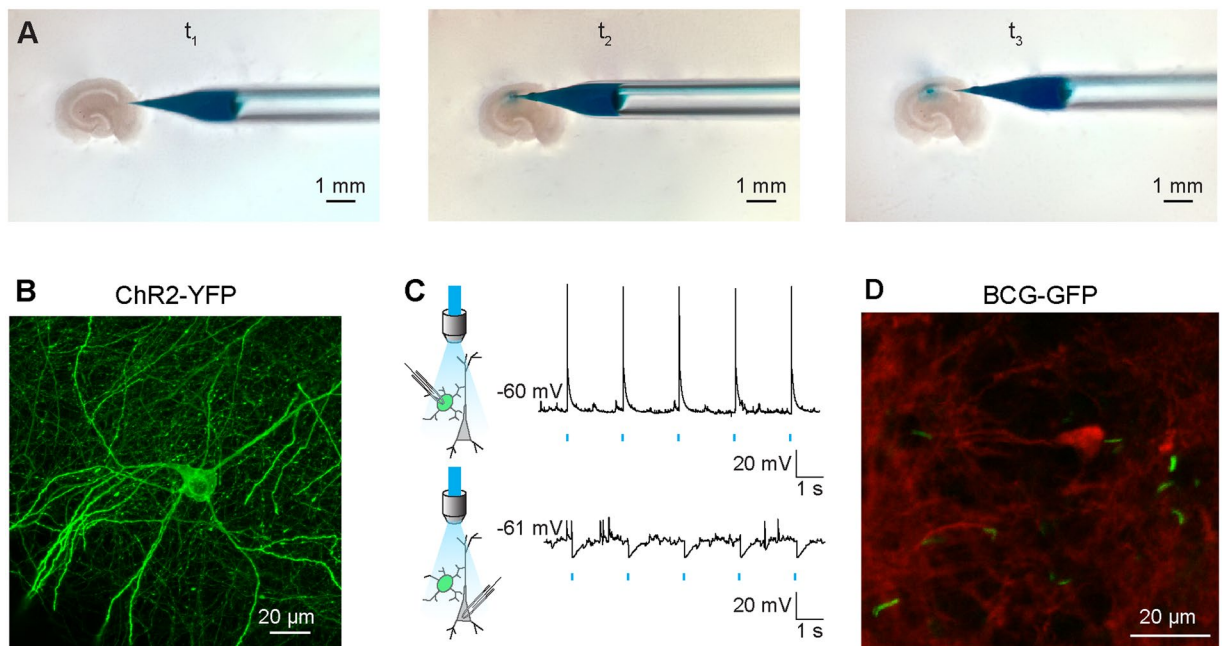


Figure 6. Openspritzer enables microinjections of infectious agents including viral delivery of opsins for optogenetics. **(A)** Openspritzer was used to perform spatially localised microinjections of infectious agents in mouse organotypic brain slices from GAD2-cre transgenic mice. At t_1 a micropipette containing AAV1 carrying floxed Channelrhodopsin2 as well as fast green (0.1%) for visualisation can be observed near the brain slice. At t_2 the glass micropipette pierced the slice surface in the CA1 area. A train of puffs triggered by a foot pedal connected to Openspritzer injected small, controlled, volumes into the brain parenchyma. At t_3 the micropipette was removed. Fast green enabled the small (200 μm diameter) inoculated area to be visualised. **(B)** Confocal image of a Channelrhodopsin2 expressing interneuron transfected as in A. **(C)** Top, whole-cell patch clamp recording from a neuron expressing ChR2. 488 nm light application using a high-powered LED results in reliable activation of action potentials confirming strong expression of Channelrhodopsin2. Bottom, recording from a nearby pyramidal cell demonstrates light evoked IPSPs confirming successful optogenetic activation of inhibitory interneurons. **(D)** Confocal image of a fixed organotypic hippocampal slice demonstrating successful infection with BCG-GFP (green). Neuronal process are visible due to staining with an antibody for β -tubulin III (red).

delivering smaller doses for a given puff duration, thus hinting at a higher control fidelity over dosage. However, the discrepancy could also be caused by small differences in pressure. Although both the input pressures were set to 1.4 bar in each experiment, the internal resistance of the pneumatics likely differed for the two systems thus resulting in a difference of absolute drug dosage. Varying the pressure is likely to change the nature of the steady state, and how quickly the steady state can build up. The second key difference is the variability of the dosage on repeated puffs. Figure 2F shows the distribution of the normalised maximum peak intensity about the mean normalised maximum intensity for both the Openspritzer and Picopump. While the overall width and shape of the distributions is very similar between the two systems, Openspritzer exhibited a longer tail than Picopump, suggesting that Openspritzer sometimes delivers higher doses for the same settings than Picopump. However, this could also be an artefact due to differences in the time delay between pulses. The automatically generated Openspritzer puffs have a one second delay between pulses which were shorter than the delay between Picopump pulses, which were set and triggered manually. Taken together our data shows that Openspritzer has comparable performance to that of Picopump.

Supporting Table 1 compares the specifications for a range of major commercial microinjectors against the specifications for Openspritzer. The measured time resolution of the Openspritzer is better than the quoted time resolutions on the market. There are, no doubt, non-technical reasons for commercial firms to avoid quoting sub 10 ms timing accuracy, even though the Picopump is technically capable of this as shown in Fig. 2.

There are several major differences in functionality between the Openspritzer and the commercial models. The first is the absence of an intermediate pressure in the Openspritzer to prevent back filling in the off state. Such a capability could be added with a second pressure regulator to port 3 of the solenoid. Another feature of some commercial spritzers is the vacuum holding capability, in which a vacuum channel can be applied to a second micropipette to hold cells in place. This capability could for example be achieved by use of a second, modified Openspritzer in tandem, in which an open input pressure line runs orthogonal within the solenoid like in a water jet eductor. A final major difference between Openspritzer and the commercial systems is complete access to the source code of the control system in the Openspritzer, which greatly increases the range of parameters for controlling the timing and duration of puffs. Some of the injectors are described as programmable but these are limited to the parameters defined by the user interface.

To demonstrate the utility of Openspritzer we performed multiple example experiments delivering agents ranging in size from single molecules to whole bacteria. Each experiment depended critically on the performance of the device. For example, by delivering controlled puffs of either glutamate or GABA, at spatial locations of our choosing, we were able to affect neuronal voltage and spiking activity in single neurons with high precision. Further, using Openspritzer we were able to confirm the effect of the benzodiazepine diazepam for positively modulating GABA_AR signalling in multiple systems including human tissue¹². Lastly, to showcase the ability of Openspritzer to acquire novel data, we used the device to observe a previously undescribed depolarizing effect of Tuberculin Purified Protein Derivative (an extract of *Mycobacterium tuberculosis*) on hippocampal neurons. The mechanisms underlying this effect remain to be explored.

An alternative strategy for delivering compounds is via iontophoresis, which uses electrical current to drive charged molecules from a pipette¹³. Although this requires relatively low cost-equipment, it is limited to the delivery of small charged molecules. A further disadvantage of this technique is that the concentration of delivered drug is typically unknown as the relative transport of drug molecules in the electrical field of the micropipette is difficult to calibrate. Whilst pressure injection, as used by Openspritzer, overcomes these issues, artefacts due to pressure changes to the tissue can occur. Nonetheless, the spatio-temporal control of reagent delivery afforded by Openspritzer is a primary feature of the device. With the emergence of a plethora of popular new techniques involving genetic manipulation of tissue and organisms, such as optogenetics and Clustered Regularly Interspaced Short Palindromic Repeats (CRISPR)^{14–17}, the demand for equipment with the functionality of Openspritzer is likely to increase. In this vein, we have demonstrated the effectiveness of Openspritzer for delivering genetic and infectious material by successfully transfecting hippocampal neurons with the light-activated channel Channelrhodopsin2 in a cell-type specific manner. This allowed us to perform neurophysiological experiments involving the selective activation of hippocampal interneurons with light.

The cost of the full Openspritzer (~£360), as compared to several thousands of pounds for a similar commercial system, makes it particularly attractive for those wishing to pursue cutting-edge techniques in low resource environments. For example, next to a suitable stereoscope and a (sometimes optional) micromanipulator, a 'spritzer' is by far the most expensive item required for the microinjection of short guide RNAs and the Cas9 protein towards genome editing by way of the ultra-low cost CRISPR/Cas9 system¹⁸.

In conclusion, we have detailed how a high-performance, low-cost, open hardware pressure ejection system can be built using off the shelf components. Openspritzer rivals the performance of commercial systems at a fraction of the cost and is likely to be of interest for a broad range of investigators working in the chemical and life sciences.

References

- Raimondo, J. V., Kay, L., Ellender, T. J. & Akerman, C. J. Optogenetic silencing strategies differ in their effects on inhibitory synaptic transmission. *Nat. Neurosci.* **15**, 1102–4 (2012).
- Ellender, T. J., Raimondo, J. V., Irkle, A., Lamsa, K. P. & Akerman, C. J. Excitatory effects of parvalbumin-expressing interneurons maintain hippocampal epileptiform activity via synchronous afterdischarges. *J. Neurosci.* **34**, 15208–22 (2014).
- Holder, N. & Xu, Q. Microinjection of DNA, RNA, and protein into the fertilized zebrafish egg for analysis of gene function. *Methods Mol. Biol.* **97**, 487–90 (1999).
- Hammond, B. & Kreulen, D. L. Gene Therapy of the Peripheral Nervous System: Celiac Ganglia. *Methods Mol. Biol.* **1382**, 275–83 (2016).
- Stark, D. A. & Kulesa, P. M. *In vivo* marking of single cells in chick embryos using photoactivation of GFP. *Curr. Protoc. cell Biol.* Chapter 12, Unit 12.8 (2005).
- Higley, M. J. & Sabatini, B. L. Calcium signaling in dendrites and spines: practical and functional considerations. *Neuron* **59**, 902–13 (2008).
- Baden, T. *et al.* Open Labware: 3-D Printing Your Own Lab Equipment. *PLOS Biol.* **13**, e1002086 (2015).
- Pearce, J. M. *Open-Source lab. Elsevier* (Elsevier, 2013).
- Euler, T. *et al.* Eyecup scope—optical recordings of light stimulus-evoked fluorescence signals in the retina. *Pflugers Arch.* **457**, 1393–414 (2009).
- Stoppini, L., Buchs, P. A. & Muller, D. A simple method for organotypic cultures of nervous tissue. *J. Neurosci. Methods* **37**, 173–82 (1991).
- Rosenegger, D. G., Tran, C. H. T., LeDue, J., Zhou, N. & Gordon, G. R. A High Performance, Cost-Effective, Open-Source Microscope for Scanning Two-Photon Microscopy that Is Modular and Readily Adaptable. *PLoS One* **9**, e110475 (2014).
- Eghbali, M., Curmi, J. P., Birnir, B. & Gage, P. W. Hippocampal GABA(A) channel conductance increased by diazepam. *Nature* **388**, 71–75 (1997).
- Curtis, D. R. Microelectrophoresis. *Phys. Tech. Biol. Res.* **5**, 144–190 (1964).
- Cong, L. *et al.* Multiplex Genome Engineering Using CRISPR/Cas Systems. *Science* (80-.). **339** (2013).
- Hwang, W. Y. *et al.* Efficient genome editing in zebrafish using a CRISPR-Cas system. *Nat. Biotechnol.* **31**, 227–229 (2013).
- Boyden, E. S., Zhang, F., Bamberg, E., Nagel, G. & Deisseroth, K. Millisecond-timescale, genetically targeted optical control of neural activity. *Nat Neurosci.* **8**, 1263–8 (2005).
- Chow, B. Y. *et al.* High-performance genetically targetable optical neural silencing by light-driven proton pumps. *Nature* **463**, 98–102 (2010).
- Blackburn, P. R., Campbell, J. M., Clark, K. J. & Ekker, S. C. The CRISPR System—Keeping Zebrafish Gene Targeting Fresh. *Zebrafish* **10**, 116–118 (2013).

Acknowledgements

We would like to thank the authors of labrigger.com and Taro Ishikawa who provided the inspiration for Openspritzer. We are grateful for stimulating conversations with P.T.M. Dragon and P. Reed concerning circuit design, Charles Harris regarding solenoid choice and Leon Lagnado for lending us a Picopump. We also thank Graham Fieggen for performing the cortical resection and the patient for donation of tissue. Funding was provided by H2020 ERC-StG NeurVisEco 677687 (T.B.), the Newton Advanced Fellowship and the Blue Brain Project (J.V.R.). We are also grateful to the International Brain Research Organisation, the Volkswagen Foundation, the Wellcome Trust, the Company of Biologists, the International Neurochemical Society, the American Physiological Society and the Cambridge Alborada Fund for providing funds towards training workshops run by TReND in Africa that contributed to the foundations of this work. TReND in Africa gUG (www.TReNDinAfrica.org).

Author Contributions

J.V.R. conceived and built the first iteration of Openspritzer. H.T. performed the GLU, GABA and optogenetics experiments. B.M. performed the BCG injection, imaging and PPD puffing experiment with input from M.J. M.J. provided reagents. R.J.B. performed the diazepam experiment. C.F. enhanced the design of the control circuit, added the Arduino functionality and designed the 3D printed chassis with input from T.B. C.F. and T.B. conducted the two-photon fluorescence experiments. C.F., T.B. and J.V.R. wrote the paper.

Additional Information

Supplementary information accompanies this paper at doi:[10.1038/s41598-017-02301-2](https://doi.org/10.1038/s41598-017-02301-2)

Competing Interests: The authors declare that they have no competing interests.

Publisher's note: Springer Nature remains neutral with regard to jurisdictional claims in published maps and institutional affiliations.



Open Access This article is licensed under a Creative Commons Attribution 4.0 International License, which permits use, sharing, adaptation, distribution and reproduction in any medium or format, as long as you give appropriate credit to the original author(s) and the source, provide a link to the Creative Commons license, and indicate if changes were made. The images or other third party material in this article are included in the article's Creative Commons license, unless indicated otherwise in a credit line to the material. If material is not included in the article's Creative Commons license and your intended use is not permitted by statutory regulation or exceeds the permitted use, you will need to obtain permission directly from the copyright holder. To view a copy of this license, visit <http://creativecommons.org/licenses/by/4.0/>.

© The Author(s) 2017